JCTC Journal of Chemical Theory and Computation

Article

pubs.acs.org/JCTC

Modeling the Partial Atomic Charges in Inorganometallic Molecules and Solids and Charge Redistribution in Lithium-Ion Cathodes

Bo Wang, Shaohong L. Li, and Donald G. Truhlar*

Department of Chemistry, Chemical Theory Center, Inorganometallic Catalyst Design Center, and Supercomputing Institute, University of Minnesota, 207 Pleasant Street S.E., Minneapolis, Minnesota 55455-0431, United States

Supporting Information

ABSTRACT: Partial atomic charges are widely used for the description of charge distributions of molecules and solids. These charges are useful to indicate the extent of charge transfer and charge flow during chemical reactions in batteries, fuel cells, and catalysts and to characterize charge distributions in capacitors, liquid-phase electrolytes, and solids and at electrochemical interfaces. However, partial atomic charges given by various charge models differ significantly, especially for systems containing metal atoms. In the present study, we have compared various charge models on both molecular systems and extended systems, including Hirshfeld, CM5, MK, ChElPG, Mulliken, MBS, NPA, DDEC, LoProp, and Bader charges. Their merits and drawbacks are compared. The CM5 charge model is found to perform well on the molecular systems, with a mean unsigned percentage deviation of only 9% for the dipole moments. We therefore formulated it for extended systems and applied it to study charge flow during the delithiation process in lithium-containing oxides used as cathodes. Our calculations show that the charges given by the CM5 charge model are reasonable and that during the delithiation process, the charge flow can occur not only on the transition metal but also on the anions. The oxygen atoms can lose a significant density of electrons, especially for deeply delithiated materials. We also discuss other methods in current use to analyze the charge transfer and charge flow in batteries, in particular the use of formal charge, spin density, and orbital occupancy. We conclude that CM5 charges provide useful information in describing charge distributions in various materials and are very promising for the study of charge transfer and charge flows in both molecules and solids.

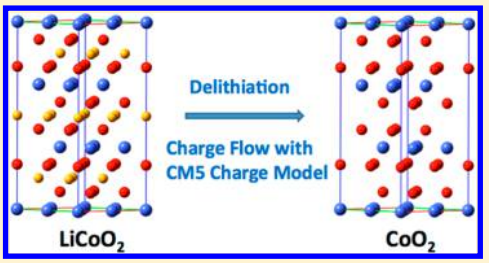

1. INTRODUCTION

A popular and powerful way to model charge distributions in molecules and solids and the electrostatic potentials they generate around molecules is by assigning a partial atomic charge to each atom in the molecule and solids, although such assignments are not unique. Partial atomic charges have been widely used to describe charge distributions within molecules and extended systems, and they can be used to gauge how much charge transfer and charge flow occurs during physical and chemical processes. For example, they are widely used for molecular dynamics simulations of proteins and nucleic acids,[1] for drug design,[2] for modeling solvation energies,[3] for quantitative structure−activity relationships,[4] and for quantitative structure−property relations.[5] They can also be used to understand the charge transfer between a metal atom and a conjugated hydrocarbon;[6] charge redistribution within copper, silver, and gold clusters;[7] charge transfer between a guest molecule and a metal−organic framework;[8] and charge transfer at water/semiconductor interfaces.[9] Another application of partial atomic charges is to understand where the electrons flow in cathodes of rechargeable lithium-ion batteries when Li atoms are extracted or inserted.[10−14] Partial atomic charges are a key quantity used to model electrostatic interactions in general.[15]

Since partial atomic charge is not a quantum mechanical observable, there is no unique way to measure partial atomic charge or to assign electron density to each atom of a molecule or solid, and various charge models[2,16−28] sometimes give significantly different partial atomic charges. Some charge models are applicable only to molecules. But, in order to study the charge distributions and charge transfers in complex systems, a charge model should give reliable partial atomic charges for both molecules and solids, and recently there has been increased interest in charge models that are applicable to both molecules and solids. In the present study, we tested various charge models on molecular systems and extended systems that contain metal atoms. We have previously found good performance of the CM5 charge model[28] in molecules, and here we extend it to solids, where we apply it to study charge flow in the delithiation of lithium-ion battery cathodes.

For a neutral molecule, the lowest nonzero moment of the molecular charge distribution is the molecular dipole moment. (For a charged species, the molecular monopole moment is nonzero but tells nothing about the charge distribution; the lowest nonzero molecular moment that provides information about the distribution of charge in the molecule is the molecular dipole moment.) One important criterion for assigning partial atomic charges is that they should yield reasonably accurate predictions for the first moments of charge distributions, i.e., for dipole moments. If one also includes

Received: July 11, 2014
Published: October 30, 2014

   dx.doi.org/10.1021/ct500790p | J. Chem. Theory Comput. 2014, 10, 5640−5650

higher multipoles on each atom, a consistent picture of the whole charge distribution will probably require different partial atomic charges than if one uses only partial atomic charges, which are the atomic monopole moments, but charge distributions that contain higher distributed multipole moments are harder to work with. Since our goal is to describe the charge distribution as simply as possible, and since partial atomic charges have a simple interpretation of electronic charge transfer between atomic centers and are of great interest because they are in widespread use in force fields, we use only the partial atomic charges. At a large enough distance from a neutral molecule, the electrostatic potential is entirely determined by the dipole moment. One can determine partial atomic charges that yield realistic electrostatic potentials not only far away but also near the van der Waals surface of molecules by fitting electrostatic potentials in the regions around molecules. But, for extended molecules with buried atoms, this procedure becomes unstable,[29] and for periodic systems, there is no external region. So we seek other methods of finding the best partial atomic charges; in particular we attempt to determine them by analyzing quantum mechanically calculated electronic wave functions and/or quantum mechanically calculated electronic charge distributions.

Partial atomic charges can also be useful for modeling solid-state materials. But for that purpose we cannot use dipole moments, and for surface science applications, fitting the electrostatic potential outside the surface of a solid is more sensitive to the surface charge distribution than to the bulk one. It is therefore hard to validate methods for predicting partial atomic charges in bulk solids. One way to proceed is to develop methods for extracting charges from quantum mechanical electronic structure calculations, to test these by comparing their predictions for dipole moments of molecules to the values calculated from the full density, and—based on this validation—to use the most accurate methods to predict partial atomic charges in solids. This is the strategy we use here. We should, however, keep in mind that we are using only partial atomic charges, not atomic dipoles, and that our goal is to predict the first moments of molecular charge distributions and electronic charge transfer between atomic centers in both molecules and solids.

CM5 charges are obtained by mapping the charges from Hirshfeld population analysis.[17] It has been shown[28] that CM5 charges predict more accurate dipole moments for molecules than Hirshfeld charges[17] or Mulliken charges, even for molecules containing transition metals, although no transition metals were used for parametrization (however, the performance was not compared to the wide variety of charge models considered here, and extended systems, such as solids, were not considered). Compared to charges obtained by electrostatic fitting,[2,18] which generally reproduce small-molecule dipole moments calculated from the electron density quite well, but have stability problems,[29] especially for buried atoms, CM5 charges are more stable and can be used in extended systems and even in the solid state.

The rest of the paper is organized as follows. Section 2 gives an overview of various charge models tested in the current study. Section 3 explains the methods and computational details. Section 4 shows the performance of various charge models and discusses the use of partial atomic charges, and section 5 summarizes the main conclusions of the present study.

2. OVERVIEW OF VARIOUS CHARGE MODELS

In the present study, we have compared Hirshfeld charges,[17] Charge Model 5 (CM5)[28] charges, Density Derived Electrostatic and Chemical (DDEC) charges,[25,26] Merz–Kollman (MK)[30] electrostatic-potential-fitting charges, CHarges from Electrostatic Potentials using a Grid (ChElPG),[31] Mulliken population analysis,[16] Mulliken charges after projecting onto a minimum basis set (MBS),[22] Natural Population Analysis (NPA),[19] charges from Local Properties (LoProp),[23] and Bader[32] charges on both molecular systems and extended systems. The basic principles of these charge models are summarized below.

Hirshfeld charges[17] are derived by partitioning the electron density into the contribution of each atom in proportion to the electron density of free neutral atoms. The Hirshfeld charge of atom A is defined as

$$q_A = Z_A - \int \mathrm{d}\mathbf{r}\, \frac{\rho_A^0(\mathbf{r})}{\sum_B \rho_B^0(\mathbf{r})}\, \rho(\mathbf{r}) \tag{1}$$

where Z_A is the nuclear charge of atom A, $\rho_A^0(\mathbf{r})$ is the spherically averaged ground state electron density of neutral atom A, and $\rho(\mathbf{r})$ is the electron density of the molecule. It has been found by several groups[26,28,33,34] that the charges yielded by eq 1 are usually smaller than those required to give good electrostatics or dipole moments (which is a special case of electrostatics since the electrostatic potential of a neutral molecule at large distance is entirely determined by the dipole moment). We also found that the underestimation of charge is relatively insensitive to basis set and is systematic and can be largely removed by a mapping in the CM5 charge model.[28] The densities $\rho_A^0(\mathbf{r})$ in eq 1 may be called prodensities or reference densities. Some proposals to improve on Hirshfeld charges involve making the prodensities functions of charge,[26,34] but we keep the simplification of using only neutral prodensities because we found in previous work that the CM5 charge models can yield good results even for charged systems with Hirshfeld charges based on only neutral prodensities.[28]

CM5 charges are derived by mapping from the Hirshfeld population analysis through the following equations.

$$q_k^{\mathrm{CM5}} = q_k^{\mathrm{HPA}} + \sum_{k \neq k'} T_{kk'} B_{kk'} \tag{2}$$

$$B_{kk'} = \exp[-\alpha(r_{kk'} - R_{Z_k} - R_{Z_{k'}})] \tag{3}$$

where q_k^{CM5} and q_k^{HPA} are the CM5 charge and Hirshfeld charge of atom k, $r_{kk'}$ is the distance between atoms k and k', $T_{kk'}$ represents parameters related to atoms k and k', and R_{Z_k} is atom k's atomic radius, which depends only on the atomic number Z_k of atom k. CM5 charges greatly improve the description of dipole moments compared to Hirshfeld charges.[28]

Density Derived Electrostatic and Chemical (DDEC) charges[25,26] are derived to reproduce chemical states of atoms and the electrostatic potentials in the system at the same time.

Merz–Kollman (MK)[30] and the CHarges from Electrostatic Potentials using Grid (ChElPG)[31] charges are electrostatic-potential-fitted (ESP fitted) charges. They are both fitted to reproduce the electrostatic potentials calculated by quantum mechanics at selected points (a "grid") and differ only in the selection of fitting points. ESP fitted charges usually reproduce the quantum mechanically calculated electrostatic potentials and dipole moments quite well and can converge with

dx.doi.org/10.1021/ct500790p | J. Chem. Theory Comput. 2014, 10, 5640–5650

increasing basis-set size. However, the equations for the charges on interior atoms in a system are ill conditioned, and the resulting charges are unstable and may have unphysical values.[29] This is a particularly troublesome feature for extended systems for which all or most atoms may be interior ones. For example, all atoms are interior in periodic calculations on solids or liquids. Most atoms are interior in periodic calcuations on liquid−vapor or solid−vapor interfaces, and even moderately sized molecules and fragments often have one or more interior atoms (such as a carbon atom in an alkyl group) that already show instability. Thus, even though electrostatic fitting yields reasonably good results for most of the small systems considered here and provides what may be considered benchmark results for very small molecules, we do not consider the method to be a viable candidate for the method of choice for extended systems. Restrained ESP (RESP) charges[35,36,24,27] involve restraining the partial atomic charges so they do not differ significantly from target values. This can improve the stability for interior atoms; however, the restraints are somewhat arbitrary since there are many choices for the target values and for how they depend on geometry, so RESP charges are not considered in the present study. The stability can also be improved by using screened electrostatics,[37] but in regions of stability the screened-ESP algorithms give similar charges to ESP charges,[37] and they will not be considered further in the present analysis.

Mulliken[16] and minimum basis set (MBS) Mulliken[22] charges are based on partitioning of the overlap matrix of atomic orbitals. Since Mulliken charges are very sensitive to the basis sets, the MBS Mulliken charge algorithm was developed to improve the partition by mapping the charge density to the minimum basis set, which gives a more balanced description among atoms and ameliorates some instability problems of Mulliken charges.[22]

Natural population analysis (NPA) charges[19] use natural bond orbitals with maximum electron density and natural atomic orbitals to localize the electrons to atoms. This reduces the basis-set dependence.

LoProp charges[23] are derived by the orthogonalization of the original basis set to get a set of localized orthonormal basis set. (This may be an improvement over the Löwdin scheme,[38,39] in that it involves three or four separate and specialized Löwdin orthonormalizations, and it may be an improvement over natural atomic orbital analysis, in that it depends only on geometry, not on electron configuration).

Bader charges[32] are based on zero-flux surfaces to divide a molecule into atoms.

The Hirshfeld and LoProp methods, as examples, can also be extended to partition other molecular properties,[23,40] but here we are concerned only with partial atomic charges.

3. METHODS AND COMPUTATIONAL DETAILS

All calculations were carried out using a combination of software packages, in particular VASP,[41,42] Gaussian 09,[43] CM5PAC,[44] CHARGEMOL,[45] BAND,[46−48] Molcas,[49,50] and BADER.[51]

All calculations in this article are for the ground electronic state of neutral molecules. The first test suite for molecular systems includes several oxides, sulfides, and hydroxides. In particular, it contains TiO_2, MnO_2, CoO_2, ZrO_2, TiS_2, Li_2S, Li_2O, FZn(OH), FMg(OH), $Zn(OH)_2$, and FMn(OH). We performed geometry optimization using Gaussian 09[43] to find the lowest energy structure; these optimizations were carried out with M06-L[52] exchange-correlation functional and the def2-TZVP[53] basis set. With the optimized ground-state geometry, partial atomic charges were calculated using various charge models. For the TiO_2, MnO_2, CoO_2, ZrO_2, TiS_2, Li_2S, and Li_2O molecules, all charge calculations were carried out with the M06-L functional and the def2-TZVP basis in Gaussian 09 except for LoProp charges, which were calculated with the M06-L functional and the ANO-RCC-VTZP[54−57] basis in Molcas. For FZn(OH), FMg(OH), $Zn(OH)_2$, and FMn(OH), M06-L/ANO-RCC-VQZP[54−57] was used for all charge models in both Gaussian 09 and Molcas, except for the FMn(OH) case in which the ANO-L-MB basis set is used for Molcas. CM5 charges were derived by using the CM5PAC program. DDEC charges with DDEC/c3 model[26] were obtained with the CHARGEMOL program, and LoProp charges were obtained by Molcas. Other charges were derived from Gaussian 09.

Among the calculations, MnO_2, CoO_2, NiO_2, TiS_2, and FMn(OH) are open-shell systems, and the others are closed-shell molecules. For the open-shell systems, we did not break the symmetry using stable = opt and nosymmetry keywords in Gaussian. MnO_2, CoO_2, NiO_2, and TiS_2 are in C_{2v} symmetry. We tested MnO_2, CoO_2, NiO_2, and TiS_2 using the stable = opt and found that, among the open-shell systems, the wave functions of CoO_2 and TiS_2 are not stable. However, for the purpose of testing partial atomic charge and to compare with different programs, we still use the nonstable wave functions to derive the charges.

The test suite for extended systems includes layered structures, $LiCoO_2/CoO_2$ and $LiTiS_2/TiS_2$; spinel structures, $Li_2Ti_2O_4/LiTi_2O_4$ and $LiMn_2O_4/Mn_2O_4$; and olivine structures, $LiMnPO_4/MnPO_4$, $LiFePO_4/FePO_4$, $LiCoPO_4/CoPO_4$, and $LiNiPO_4/NiPO_4$. The solids tested have neutral unit cells, and only ferromagnetic and nonmagnetic phases are considered. The systems are optimized using VASP. For the $LiCoO_2/CoO_2$, $LiTiS_2/TiS_2$, $LiMn_2O_4/Mn_2O_4$, and $Li_2Ti_2O_4/LiTi_2O_4$, we used M06-L optimized geometries with a 500 eV cutoff energy and $6 \times 6 \times 6$ k points; for other structures, we used PBE[58] optimized geometries with a 500 eV cutoff energy and $4 \times 4 \times 4$ k points. Standard PBE PAW potentials[59,60] provided in the package were used in all calculations. Except in a couple of places where indicated otherwise, spin polarization was included in all calculations. Both the coordinates of atoms and lattice constants were optimized.

In the original CM5 paper, only finite systems were tested.[28] However, since the charge correction is dependent on the bond order $B_{kk'}$ in eq 2, and the bond order exponentially decreases with respect to the distance between atoms, only several nearby atoms are needed to get a converged CM5 charge. To do CM5 charges for periodic systems, we derived Hirshfeld charges in a unit cell from the BAND program and created a cluster that includes several nearby unit cells, and we used the CM5PAC program to derive the CM5 charges of the cluster. The size of the cluster (usually $3 \times 3 \times 3$ unit cells) is chosen to make sure that the CM5 charges in the middle unit cell are converged. DDEC/c3 charges of the extended systems were calculated using the CHARGEMOL program.

In the VASP and BAND calculations, we found that several cases, including $LiTiS_2$, $Li_2Ti_2O_4$, $LiTi_2O_4$, and $NiPO_4$, have a noninteger difference between numbers of alpha and beta electrons when the electronic structure is relaxed using the M06-L functional. For these cases, M06-L predicts no band gap. We did not add spin multiplicity constraints on the extended (solid) systems, and partial occupancy of orbitals was

Table 1. Dipole Moments (in debye) of Several Gas-Phase Oxides and Sulfides Calculated from Various Charge Models and from the Full Density[a]

	TiO_2	MnO_2	CoO_2	NiO_2	ZrO_2	TiS_2	Li_2S	MUD	MUPD
multiplicity	1	4	2	5	1	5	1		
angle of molecule	112	132	125	140	108	115	144		
Hirshfeld	4.03	1.77	1.57	1.44	4.73	3.71	2.61	1.67	37%
CM5	6.32	2.91	2.57	2.05	7.54	5.49	3.29	0.34	9%
DDEC	8.65	3.31	2.75	2.51	9.93	7.05	5.93	1.25	26%
MK	6.82	2.57	2.38	2.39	8.12	5.34	4.74	0.24	7%
ChElPG	6.87	2.64	2.40	2.38	8.40	5.52	4.70	0.30	8%
Mulliken	5.64	3.48	3.38	2.32	6.91	6.85	3.86	0.84	20%
MBS	3.47	3.03	3.14	2.35	4.45	2.63	1.09	1.93	38%
NPA	6.55	3.23	2.95	2.75	8.91	5.59	5.10	0.59	15%
LoProp	5.75	4.10	4.04	*b*	6.45	*b*	4.81	1.42	40%
Bader	8.91	4.96	4.70	3.58	10.58	10.02	5.56	2.39	59%
density (Gaussian)	6.85	2.58	2.55	2.60	7.94	5.36	3.69	0.00	
density (Molcas)	6.87	2.49	2.43	*b*	7.93	*b*	3.52	0.00	

[a]The last two columns give the mean unsigned deviation (MUD) and mean unsigned percentage deviation (MUPD) of the dipole moments from density dipole moments. [b]Calculation in Molcas is not available.

allowed to increase efficiency,[61] but we checked in some cases that adding spin constraints makes only a small difference in the charge analysis.

One can derive Hirshfeld charges either from BAND or from VASP by using CHARGEMOL. However, BAND calculations are more consistent since the charge densities of neutral atoms are calculated at the same level as that for the whole molecule in BAND. Therefore, BAND is used for Hirshfeld analysis (and hence also for CM5). However, we compared the Hirshfeld charges derived from BAND to those derived from VASP and CHARGEMOL for eight solids, and we found that the difference is small, with an average difference of only 0.02*e*.

The Bader charges of atoms in molecules were calculated with Gaussian09 and BADER, and the Bader charges for atoms in solids were calculated with the VASP and BADER programs. In some molecular cases, we found the sum of the calculated partial atomic Bader charges of molecules does not equal to the total charge of the molecule, and we evenly distributed the extra charge (usually 0.1−0.2*e*) to all atoms in the molecule.

For discussion, we also calculated the partial atomic magnetization on the atoms in the molecules and solids. This is defined as the number of α electrons minus the number of β electrons on a given atomic center where these numbers are obtained using the same methods as used for partial atomic charges (which are summed over spins).

4. RESULTS AND DISCUSSION

4.1. Comparison of Various Charge Models in Small Molecules. Table 1 shows dipole moments for TiO_2, MnO_2, CoO_2, NiO_2, ZrO_2, TiS_2, and Li_2S as calculated using various charge models. The multiplicity ($2S + 1$, where S is total electron spin) and bond angle of the molecules are also shown in Table 1. The dipole moments calculated from the full electron density of the quantum mechanical calculations (labeled "density" dipoles) are assumed to be realistic and are used to measure the performance of various charge models, and mean unsigned deviation and mean unsigned percentage deviation were calculated for each charge model. Since the Gaussian and Molcas calculations use different basis sets, there is a difference between the density dipole moments from these two programs; therefore density dipole moments from Molcas are used for calculating the deviations of LoProp charges, and density dipole moments from Gaussian are used for the deviations of other charge models.

Table 2. Charges on the Metal Atoms for Several Gas-Phase Oxides from Various Charge Models, As Compared to Dipole Charges and Oxidation States

	TiO_2	MnO_2	CoO_2	NiO_2	ZrO_2
Hirshfeld	0.91	0.56	0.44	0.52	0.94
CM5	1.43	0.93	0.72	0.74	1.50
DDEC	1.95	1.05	0.77	0.90	1.98
MK	1.54	0.82	0.67	0.86	1.62
ChElPG	1.55	0.84	0.68	0.86	1.67
Mulliken	1.27	1.11	0.95	0.84	1.38
MBS	0.78	0.97	0.88	0.85	0.89
NPA	1.48	1.03	0.83	0.99	1.78
LoProp	1.30	1.31	1.13	*a*	1.29
Bader	2.01	1.58	1.32	1.29	2.11
dipole charge (Gaussian)	1.54	0.82	0.72	0.94	1.58
dipole charge (Molcas)	1.55	0.79	0.68	*a*	1.58
oxidation state	4	4	4	4	4

[a]Calculation in Molcas is not available.

Table 1 shows that the CM5 charge model performs much better than the MBS, NPA, DDEC, and LoProp charge models at reproducing the density dipole moments. The mean unsigned percentage deviation is only 9% for CM5, while most of other charge models, except for ESP fitted charge models, give a deviation greater than 15%. For molecules, the CM5 charge model performs equally as well with the electrostatic potential fitted charge models including MK and ChElPG, but it suffers no stability problems in the solid-state calculations.

Since all the molecules are triatomic and symmetric, we can directly calculate the charges that reproduce the quantum mechanical dipole moments, and we call them dipole charges. Table 2 shows both the dipole charges on metal atoms in oxides and also the charges computed from various charge models. The table shows that the charges on the metal atoms, either from the dipole moments or from any charge model, are much smaller than their oxidation states. For example, in the case of TiO_2, the Ti atom, with an oxidation state of 4, has a dipole charge of +1.54. The point of showing the oxidation

dx.doi.org/10.1021/ct500790p | J. Chem. Theory Comput. 2014, 10, 5640−5650

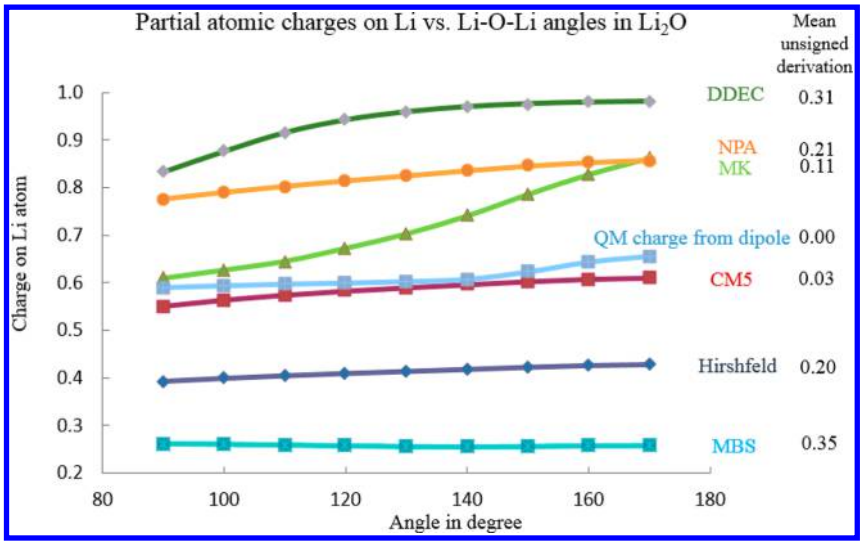

Figure 1. Partial atomic charges on Li atoms with different Li−O−Li angles in singlet Li_2O molecules using various charge models.

Table 3. Dipole Moments (in debye) of Several Gas-Phase Metal Hydroxides Calculated from Various Charge Models[a]

	FZn(OH)	FMg(OH)	$Zn(OH)_2$	FMn(OH)	MUD	MUPD	MUDD (degree)
multiplicity	1	1	1	6			
Hirshfeld	1.31	1.26	1.08	1.38	0.63	34%	6
CM5	1.95	1.65	2.18	1.97	0.16	9%	8
MK	1.90	1.97	2.01	2.07	0.10	5%	6
ChElPG	1.96	1.96	2.06	2.04	0.11	6%	6
Mulliken	3.82	4.86	4.72	4.25	2.52	134%	12
MBS	2.35	2.18	2.24	2.42	0.40	21%	1
NPA	2.74	2.14	3.41	2.68	0.85	45%	16
LoProp	2.30	1.75	2.62	1.79	0.37	20%	8
density (Gaussian)	1.88	1.88	1.84	1.97			
density (Molcas)	1.88	1.88	1.84	1.93			

[a]Mean unsigned deviation (MUD) and mean unsigned percentage deviation (MUPD) of the dipole moments (debye) obtained by using different charge models compared with the density dipole moment are shown. The mean unsigned deviation of the direction (MUDD) of dipole moments is averaged over the cases of FZn(OH) and FMn(OH). The other two molecules are linear.

Table 4. Averaged CM5 Charges of Li, Transition Metals, and Anions in Various Solid-State Materials Using M06-L[a]

	space group	$n_\alpha - n_\beta$	Li	transition metal	anion
$LiCoO_2$	$R\bar{3}m$	0	0.50	0.68	−0.59
CoO_2	$R\bar{3}m$	1		0.77	−0.38
$LiTiS_2$	$P\bar{3}m1$	0.77	0.29	0.64	−0.47
TiS_2	$P\bar{3}m1$	0		0.73	−0.36
$Li_2Ti_2O_4$	$Fd\bar{3}m$	0.48	0.49	1.06	−0.78
$LiTi_2O_4$	$Fd\bar{3}m$	0.46	0.50	1.23	−0.74
$LiMn_2O_4$	$Fd\bar{3}m$	7	0.48	0.93	−0.58
Mn_2O_4	$Fd\bar{3}m$	6		0.97	−0.48
$LiFePO_4$	$Pnma$	4	0.55	0.75	−1.30
$FePO_4$	$Pnma$	5		1.01	−1.01
$LiMnPO_4$	$Pnma$	5	0.54	0.78	−1.31
$MnPO_4$	$Pnma$	4		0.99	−0.99
$LiCoPO_4$	$Pnma$	3	0.56	0.71	−1.27
$CoPO_4$	$Pnma$	4		0.91	−0.91
$LiNiPO_4$	$Pnma$	2	0.55	0.91	−1.46
$NiPO_4$	$Pnma$	1.50		0.99	−0.99

[a]The space group of the materials is shown in the first column. Difference between number of α and β electrons per formula unit is shown on the second column.

state is not just that the oxidation state does not match the partial atomic charge, which is well-known to many workers for at least some substances, but that a change in oxidation state is not necessarily accompanied by a significant change in partial atomic charge, and it cannot be used to study charge flow. We will discuss this more in section 4.3.1. Table 2 also shows that in general Hirshfeld and MBS give charges that are smaller, and NPA and DDEC give charges that are larger than charges that give accurate first moments of the charge distributions.

Figure 1 shows the charges on Li atoms in Li_2O with various Li−O−Li angles as obtained using several charge models. For each point in the plot, the bond length of Li−O is optimized with a fixed Li−O−Li angle. A more complete set of data is shown in Table S1 in the Supporting Information. Figure 1 and Table S1 show that CM5 and Mulliken charges correctly describe the charges for various Li_2O conformations, which is a success not achieved by other charge models.

Table 3 shows results for several metal hydroxides, and again the CM5 charges perform as well as ESP-fitted charges and better than other kinds of charge models. Table 3 shows a serious breakdown of the Mulliken charge model, which is not surprising since the Mulliken model is known to be unreliable in the general case for extended basis sets; in contrast, the CM5 charge model has given consistently reasonable results, making

Table 5. Averaged CM5 Charges of Li, the Other Metal, and O for $Li_2Ti_2O_4$, $LiTi_2O_4$, and $LiMn_2O_4$ Using M06-L and HSE06

	M06-L, BAND			M06-L, VASP, and CHARGEMOL			HSE06, VASP, and CHARGEMOL		
	Li	metal	O	Li	metal	O	Li	metal	O
$Li_2Ti_2O_4$	0.49	1.06	−0.78	0.48	1.07	−0.78	0.48	1.08	−0.79
$LiTi_2O_4$	0.50	1.23	−0.74	0.50	1.24	−0.74	0.49	1.25	−0.75
$LiMn_2O_4$	0.48	0.93	−0.58	0.49	0.89	−0.56	0.50	0.92[a]	−0.58

[a]Mn atoms at different sites have different partial atomic magnetization in this calculation, and the charge is 0.98 at one site and 0.86 at the other.

Table 6. Averaged CM5 Charge Flow on Metal Atoms and Anions during Delithiation in Various Solid-State Materials Using M06-L

	transition metal	anion
$LiCoO_2$	0.08	0.21
$LiTiS_2$	0.09	0.11
$Li_2Ti_2O_4$	0.17	0.04
$LiMn_2O_4$	0.04	0.10
$LiFePO_4$	0.26	0.29
$LiMnPO_4$	0.21	0.32
$LiCoPO_4$	0.20	0.36
$LiNiPO_4$	0.08	0.47

it our leading candidate for the study of charge flow in lithium-ion battery cathodes, which will be studied in the next section.

Overall, the CM5 charge model performs well on neutral molecules that contain metal atoms. It will be tested on extended systems in the next section.

4.2. Charge Models in Solid-State Systems and Charge Flow during Delithiation. After the CM5 charge model was validated on small molecules, we applied it to extended systems, in which no unambiguous charge on atoms can be assigned. We also calculated Hirshfeld charges, Mulliken charges, DDEC, and Bader charges to make a comparison. We do not show the ESP-fitted charges for extended systems since atoms are buried, and we found (as expected) that the ESP-fitted charges can be very unphysical.

Table 4 shows the CM5 charges of atoms in these materials, including the lithiated and delithiated forms. The phases we tested are shown in the first column of the table. The difference between the number of α electrons and the number of β electrons per formula unit for each solid is also shown in the table.

In most of the materials, the Li atom has a charge of ~0.5, which is similar to the CM5 charge on Li in Li_2O. The only exception is $LiTiS_2$, which has less positive Li ions. This is due to the high covalent character of the $LiTiS_2$ structure. Another interesting finding is that although some atoms may have the same oxidation states in two compounds, their charges can be significantly different. For example, Ti atoms have a charge of 0.64 in $LiTiS_2$ and a charge of 1.06 in spinel $Li_2Ti_2O_4$.

A possible concern with the present calculations is that M06-L and other local functionals usually underestimate the band gap and can predict that some materials are conductors when actually they are insulators. A second concern is that only the ferromagnetic and nonmagnetic phases are tested. However, we found in selected test cases that the Hirshfeld and CM5 charges are insensitive to the phases and magnetic moments of the compounds. We provide three illustrations of this: (i) HSE06[62] correctly predicts that $Li_2Ti_2O_4$ and $LiTi_2O_4$ are semiconductors with a band gap around 0.6 eV, whereas M06-L

Table 8. Averaged CM5 Charges of Li, Co, and O Atoms in Solid-State Li_xCoO_2

X	Li	Co	O
1.0	0.50	0.68	−0.59
0.5	0.58	0.75	−0.52
0.0		0.76	−0.38

Table 9. Natural Electron Configuration of the Metal Atoms in Metal Oxide Molecules

	dipole charge	NPA charge	natural electron configuration
TiO_2	1.54	1.48	4s (0.04), 3d (2.37), 4p (0.14)
MnO_2	0.82	1.03	4s (0.38), 3d (5.28), 4p (0.31)
CoO_2	0.72	0.83	4s (0.42), 3d (7.48), 4p (0.27)
NiO_2	0.94	0.99	4s (0.33), 3d (8.45), 4p (0.22)
ZrO_2	1.58	1.78	5s (0.04), 4d (2.14), 5p (0.10)

Table 10. Averaged Hirshfeld Partial Atomic Magnetization on Metal Atoms and Nonmetal Atoms in Various Solids

	transition metal	anion
$LiCoO_2$	0.00	0.00
CoO_2	0.93	0.03
$LiFePO_4$	3.67	0.32
$FePO_4$	4.20	0.80

Table 7. Averaged Hirshfeld, Mulliken, DDEC, and Bader Charges of Li Atoms, Transition Metal Atoms, and Nonmetal Atoms in Various Solid-State Materials Using M06-L

	Hirshfeld			Mulliken			DDEC			Bader		
	Li	transition metal	anion	Li	transition metal	anion	Li	transition metal	anion	Li	transition metal	anion
$LiCoO_2$	0.14	0.32	−0.23	0.81	1.12	−0.96	1.00	1.45	−1.23	0.87	1.28	−1.08
CoO_2		0.34	−0.17		1.35	−0.67		1.23	−0.62		1.50	−0.75
$LiTiS_2$	0.09	0.25	−0.17	−0.15	−1.08	0.62	0.97	1.48	−1.23	0.87	1.54	−1.20
TiS_2		0.29	−0.14		−0.79	0.39		1.06	−0.53		1.68	−0.84
$Li_2Ti_2O_4$	0.15	0.48	−0.32	0.59	1.35	−0.97	1.00	2.10	−1.55	0.87	1.74	−1.30
$LiTi_2O_4$	0.20	0.57	−0.34	0.90	1.70	−1.07	1.00	2.32	−1.41	0.89	1.92	−1.18
$LiMn_2O_4$	0.16	0.48	−0.28	0.81	1.55	−0.98	1.00	1.95	−1.23	0.87	1.75	−1.10
Mn_2O_4		0.47	−0.23		1.64	−0.82		1.47	−0.73		1.80	−0.90

dx.doi.org/10.1021/ct500790p | J. Chem. Theory Comput. 2014, 10, 5640−5650

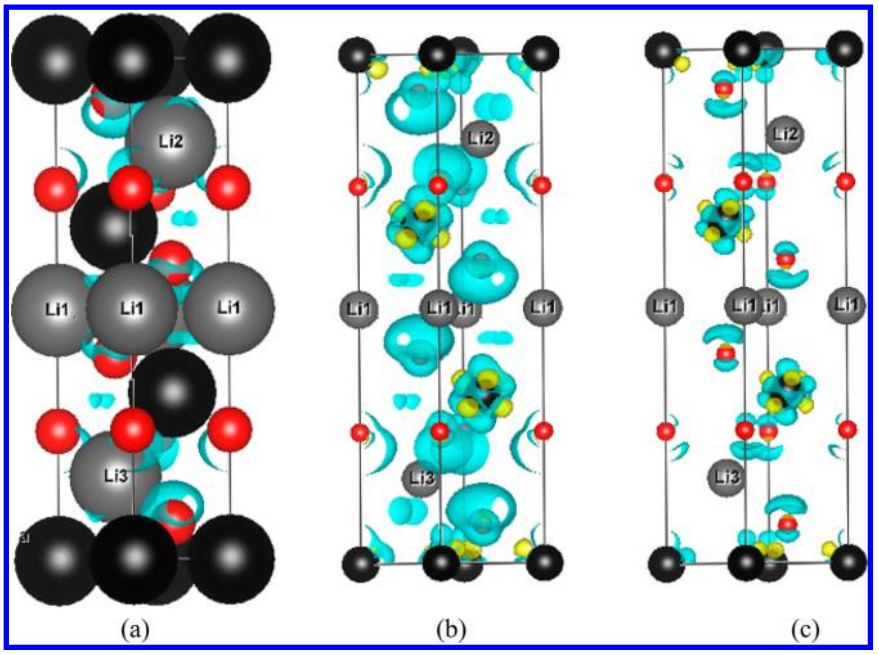

Figure 2. Isosurfaces of the electron density difference between CoO_2 and $LiCoO_2$ using the M06-L functional. Yellow and blue represent positive (electron gained) and negative (electron depleted) (a, b) 0.0075e/Å^3 isosurfaces and (c) 0.015 e/Å^3 isosurfaces, respectively. Part a uses space filling representation with covalent radii of atoms to show the size of atoms. Oxygen atoms are represented by red balls, Co atoms by black balls, and Li atoms by gray balls. Three formula units are shown in the figures. All the lithium atoms are deleted in CoO_2 to make a comparison. Although in the experiment, only 0.5 Li atom is removed from $LiCoO_2$, we tested the electron density change for the fully delithiated one, CoO_2.

Table 11. Partial Atomic Charges on the Metal Atoms (the Middle Mg atom for MgOMgO Case)

	MgO	MgOMgO	MgO^+	CaO	CoO_2^+	Mn_2O_7	ScOF	VO_3	CaF_2 (bent)
Hirshfeld	0.58	0.66	1.31	0.58	0.94	0.56	1.07	0.52	0.84
CM5	0.75	0.94	1.45	0.90	1.27	1.27	1.46	1.20	1.12
MK	0.78	1.18	1.62	0.95	1.25	0.74	1.58	1.46	1.47
DDEC	0.97	1.62	1.73	1.18	1.36	1.79	2.02	2.25	1.69
dipole charge	0.75		1.62	0.93	1.44				1.48

Table 12. Dipole Moment (in debye) Calculated by Various Charge Models and the Full Density[a]

	MgO	MgOMgO	MgO^+	CaO	CoO_2^+	Mn_2O_7	ScOF	VO_3^-	CaF_2 (bent)	**MUD (Table 11)**	**MUD (Tables 1 and 11)**
Hirshfeld	4.86	8.87	6.18	5.10	0.79	0.08	0.32	0.00	1.41	**1.36**	**1.50**
CM5	6.28	10.23	7.41	7.88	1.61	0.20	1.70	0.00	1.88	**0.52**	**0.44**
MK	7.28	10.95	8.89	8.34	1.54	0.36	1.04	0.01	2.47	**0.24**	**0.24**
DDEC	8.06	12.18	9.81	10.38	1.78	0.11	1.81	0.01	2.84	**0.89**	**1.05**
Density	7.01	9.87	8.92	8.14	2.03	0.34	1.09	0.00	2.50	**0.00**	**0.00**

[a]The last two columns give the mean unsigned deviation (MUD) of the dipole moments from density dipole moments.

predicts no band gap. Table 5 shows the comparison of CM5 charges using the various methods (because one can derive Hirshfeld charges (and therefore CM5 charges) from BAND or from Chargemol, we show both results). We found that the CM5 charges change only a little when using HSE06 to open the band gap. This shows that Hirshfeld charges and CM5 charges are not sensitive to the predicted band gap. (ii) HSE06 also correctly predicts the charge disproportionation state of $LiMn_2O_4$ in which Mn atoms at different sites are not equivalent,[63] whereas M06-L predicts a symmetric structure in which they are equivalent. Table 5 shows that although the partial atomic magnetization on the Mn atoms differs by about 1.0, the CM5 charges at the two Mn sites differ only by 0.12, and the averaged CM5 charges on Li, Mn, and O atoms are similar (the same within 0.03) to the noncharge-disproportionated state. (iii) The results in Table 4 are ferromagnetic; i.e., all the unpaired spins are aligned. We also tested $LiMn_2O_4$ and $LiFePO_4$ with antiferromagnetic states (the unit cells of these two solids contain four metal atoms), and the Hirshfeld charges are very similar to those for the ferromagnetic states (differences about 0.01).

To better understand how charge flows during the delithiation process, we compared the lithiated and delithiated materials, and we calculated the charge difference on the transition metal atoms (Ti, Co, Ni, Fe, or Mn) and the anions (O, S, or PO_4). The difference is called the charge flow, and the results are shown in Table 6. Table 6 shows that charge flow occurs on both the transition metal and the anion (O or S or PO_4). In certain cases, the charge flow happens mostly on oxygen atoms. This is not generally recognized in the study of lithium-ion batteries, where the oxidation states are usually used

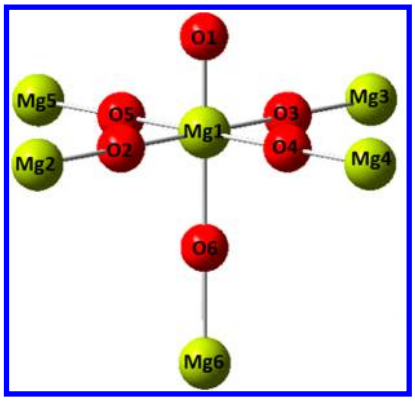

Figure 3. $(MgO)_6$. Mg1−O1 bond length is 1.67 Å, and all other Mg−O bond lengths are 2.02 Å. Cluster $(MgO)_x$ ($x = 1 - 6$) only contains atoms Mg1−Mgx and O1−Ox labeled in the figure.

Table 13. Partial Atomic Charges on the Central Mg Atom in Magnesium Oxide Clusters (Labeled Mg-1 in Figure 3)

	MgO	$(MgO)_2$	$(MgO)_3$	$(MgO)_4$	$(MgO)_5$	$(MgO)_6$
Hirshfeld	0.59	0.69	0.56	0.42	0.28	0.15
CM5	0.79	0.97	0.93	0.88	0.82	0.77
DDEC	1.00	1.55	1.72	1.76	1.79	1.84

as indicators of the charge distribution, and only the metal atoms are considered to be oxidized in the delithiation process.

To make comparisons between charge models, Table 7 shows the Hirshfeld charges, Mulliken charge, DDEC charges, and Bader charges on several solid-state systems. The Hirshfeld and CM5 charges are generally smaller than Mulliken and DDEC charges for the cases and basis sets that we study here. From the tests on molecular systems, we already know that the Hirshfeld method usually gives charges that are too small. For the Mulliken charges, we found unphysical charges for $LiTiS_2$ and TiS_2 compounds, which may be attributed to the instability of Mulliken charges with large basis sets. Also Mulliken charges are very sensitive to the basis sets, as mentioned in section 2 of the paper. As for the DDEC charges, they are closer to the formal charges of the atoms. For example, the Li atom usually has a DDEC charge of +1. We found that sometimes the DDEC charges may not be stable enough to be used for comparison between different materials. For example, in the delithiation process of $LiCoO_2$, $LiTiS_2$, and $LiMn_2O_4$, the DDEC charges lead to the interpretation that the transition metals are reduced and become less positive, while the oxygen atoms are oxidized. This does not agree with traditional experience or chemical intuition. To summarize the comparisons between CM5 charges and Mulliken and DDEC charges, we found that the CM5 charge model predicts smaller partial atomic charges than the DDEC charge models, that the CM5 charges are more stable than Mulliken and DDEC charges, and that CM5 charges give reasonable results for charge transfer and charge flow in various materials.

To further study the charge flow in the $LiCoO_2$ delithiation process, a partially delithiated compound, $Li_{0.5}CoO_2$ in the $P2/m$ space group,[64] was tested and compared with $LiCoO_2$ and CoO_2, with the results shown in Table 8. Only spin-unpolarized results for the three cases $LiCoO_2$, $Li_{0.5}CoO_2$, and CoO_2 are shown in Table 8. (The numbers of α and β electrons are the same in the three cases here, while they are not the same in the CoO_2 case shown in Table 4.) A more detailed discussion about spin polarization will be presented in section 4.3.2. We found that the charge flow is equally distributed on Co and O atoms when x changes from 1.0 to 0.5 and occurs mostly on O atoms when x changes from 0.5 to 0.0. This phenomenon indicates that when x is less than 0.5, the charges on O atoms can decrease significantly. This is consistent with the experimental result that the O atoms are being oxidized for deeply delithiated $LiCoO_2$.[65]

4.3. Comparison of Other Approaches to Determine Charge Flow. *4.3.1. Oxidation State.* A very simple way to assign partial atomic charge in the solids is to use the oxidation states (or formal charges) of the atoms. For example, when considering the delithiation of $LiCoO_2$ solid to CoO_2 solid, it is sometimes assumed that the Co atom changes its charge from +3 to +4, while the oxygen atom keeps its charge at −2. This approach oversimplifies the description of charge distributions.

Formal assignment of the number of d electrons, which is also common in discussing transition metal chemistry, is also unphysical. The covalent character of the bonds is not taken into consideration. Table 9 shows the electron occupancy in atomic orbitals of metal atoms in several metal oxide molecules using natural population analysis[19] (Although NPA usually gives charges that are too large, as shown in Table 1, it gives useful information about orbital character and trends of charge distributions among various molecules.) The NPA analyses in Table 9 show that the s and p atomic orbitals are significantly populated, especially for Mn, Co, and Ni in our test.

4.3.2. Spin Density. Another way to look at the charge distribution is to use the partial atomic magnetization at each atomic center.[66] Table 10 shows the partial atomic magnetization on metal atoms and anions (oxygen or PO_4) in solid-state $LiCoO_2$, CoO_2, $LiFePO_4$, and $FePO_4$. In $LiCoO_2$ and CoO_2 solids, our calculations show that the net spin is mainly localized on the Co center, and the partial atomic magnetization of the Co atom changes from 0 to 0.9 when $LiCoO_2$ is delithiated to CoO_2. However, this does not necessarily indicate that there is a transfer of one electron on the Co atom. We compared spin polarized and spin-unpolarized calculations with the same total numbers of electrons on CoO_2. In the spin polarized calculation, the numbers of α electrons and β electrons are allowed to change, and there is one more α electron than β electron in each formula unit, while the numbers of α and β electrons are kept the same in the spin-

Table 14. Dipole Moment (in debye) Calculated by Various Charge Models and the Full Density[a]

	MgO	$(MgO)_2$	$(MgO)_3$	$(MgO)_4$	$(MgO)_5$	$(MgO)_6$	MUD
Hirshfeld	4.76	5.00	3.25	5.29	2.24	5.02	**1.05**
CM5	6.37	6.45	4.86	6.27	3.85	6.64	**1.60**
DDEC	8.06	8.40	6.30	6.52	4.54	7.84	**2.62**
Density	6.89	5.90	3.54	4.32	1.23	4.04	**0.00**

[a]The last column gives the mean unsigned deviation (MUD) of the dipole moments from density dipole moments.

unpolarized calculation. We found that the Hirshfeld partial atomic charges from the spin-polarized and spin-unpolarized calculations are very similar. The Mulliken partial atomic charges from these two calculations are also similar. However, these two calculations give completely different partial atomic magnetization on Co (the partial atomic magnetization on Co is 0 in spin-unpolarized calculations). Changing the spin may change the relative occupancy of α and β electrons without changing the overall charge distribution of atoms.[67] On the basis of their ability to predict the first moments of charge distributions, we believe the partial atomic charges are a more reliable way to describe the charge transfer than the partial atomic magnetization.

4.3.3. Charge Density. One can understand the charge redistribution or charge flow from the charge density change. This has an advantage over the use of partial atomic charges since the charge density is a physical observable. The charge density change and electron density change differ by the sign, and we use electron density change in the following discussion. The electron density difference between the lithiated and delithated materials is defined as

$$\rho(\text{diff}) = \rho(\text{delithated}) - \rho(\text{lithiated}) \quad (4)$$

Figure 2 shows the electron density change for the delithiation of $LiCoO_2$ to CoO_2 with $0.0075e/Å^3$ and $0.015\ e/Å^3$ isosurfaces. Figure 2a uses space filling representation with covalent radii of atoms to show the size of atoms. The figure clearly shows that both the oxygen atoms and the Co atoms lose electrons during the delithiation, which is consistent with the changes in the CM5 partial atomic charges. It seems that there is little electron density change around the Li nuclear center in Figure 2b and c ($1s^2$ electrons are represented by a PAW potential and are not included in the plots of Figure 2). However, comparing Figure 2a, which shows the sizes of atoms with covalent radii, and Figure 2b, we found that parts of the $0.0075e/Å^3$ isosurfaces are within the Li region, indicating that the electron density does change in the regions around the Li nuclear center. This is consistent with our conclusion that the Li atoms have a charge of less than +1. Although the charge density contains the complete description of how the electrons distribute in the system, partial atomic charges are easier to use, especially in complex systems where the charge density can be too complicated to analyze in a useful way.

4.3.4. Tests on Systems with High Partial Atomic Charges. Since Charge Model 5 (CM5) is based on the Hirshfeld analysis that uses neutral reference atoms, one might question whether CM5 charges work well with high partial atomic charges (i.e., charge distributions that differ significantly from neutral atoms). In previous work,[28] we have shown that the CM5 charge models can yield good results even for charged systems; in fact we obtained more accurate dipole moments for charged system than are obtained by the iterative Hirshfeld scheme[34,68] that does use ionic reference densities. We concluded that neutral atomic reference densities were sufficient, and they also have the advantage of being unambiguous and not requiring self-consistent iterations. Here, we further test this conclusion for a second test suite of systems containing metal atoms. We consider the following systems, most of which were chosen in order to test the method for cases where the partial atomic charges were expected to be higher than in the cases considered earlier in the paper. In particular, we consider gas-phase MgO, MgOMgO, MgO^+, CaO, CoO_2^+, VO_3^-, Mn_2O_7, ScOF, and CaF_2. M06-L/def2-TZVP was used to optimize the geometries. Charge analysis was carried out for the optimized geometries with M06-L/def2-TZVP, except for CaF_2, in which we bent the F−Ca−F angle to 160° and kept the F−Ca distance at the optimized bond length for the linear species. Tables 11 and 12 show the partial atomic charges and dipole moments predicted by various charge models and the quantum mechanically calculated dipole moments. We did find that our chosen systems can have larger partial atomic charges, as shown in Table 11, and we found—as expected—that Hirshfeld analysis gives systematically too small charges that underestimate the first moments of the charge distributions, as indicated by the dipole moments. However, the CM5 charge model corrects the systematic deviation of Hirshfeld analysis and gives reasonable dipole moments (first moments of the charge distributions) even in these systems with highly uneven charge distributions. In contrast, Density Derived Electrostatic and Chemical (DDEC) gives charges and dipole moments that are typically larger. We give two MUD columns, one for the molecules in Table 11 and one for the union of the sets of molecules in Tables 1 and 11. The MUD of CM5 is about the same in both columns. Merz−Kollman (MK) ESP fitted charges can reproduce the dipole moments quite well. However, as we mentioned before, ESP fitted charges suffer from the instability problem for the interior atoms.

Solid-state MgO is a case where attempts have been made to obtain the partial atomic charges experimentally, as reviewed by Zuo,[69] who commented that "The charge transfer only affects a few low-order structure factors and is difficult to measure... Similarly, in the case of often-cited textbook evidence for ionic bonding, the experimental NaCl electron density has an uncertainty in the measured structure factors which is far larger than the difference between models consisting of neutral atoms or ions." Furthermore, the extraction of partial atomic charges from experimental data involves assumptions very similar to the extraction of partial atomic charges from wave function densities, for example, truncated multipolar expansions and spherical pseudoatoms that are expanded and contracted to fit the data. A recent paper[26] concluded that "further improvements are needed to make extracting accurate net atomic charges from experimental data a routine procedure." We therefore undertook the study of MgO molecules. We already showed results for MgO and MgOMgO. Finally, we tested a series of gas-phase clusters $(MgO)_x$ (x = 1−6) with M06-L/def2-TZVP single-point calculations to see how the charge of the central Mg atom changes when it is surrounded by more and more MgO units. The structure for x = 6 is shown in Figure 3; it is slightly asymmetrical to yield a nonsymmetry-determined first moment that can be used to test charge models. The clusters were created by starting with the fixed geometry with x = 6 (bond lengths shown in the caption of Figure 3), then removing the MgO unit labeled with Mg-6, then removing the Mg−O unit labeled with Mg-5, etc. Tables 13 and 14 show the partial atomic charges of the central Mg atoms and dipole moments predicted by various charge models. It is found that both CM5 and DDEC charge models predict larger dipole moments than the quantum mechanical dipole moments. The DDEC model predicts a high charge for the central Mg, but the lower charges predicted by CM5 yield more accurate first moments of the charge distribution.

5. CONCLUSIONS

In the present study, we have compared several charge models to derive the partial atomic charges of inorganometallic

molecules and solids. The CM5 charge model is validated on a set of small molecules containing transition metals. The CM5 charges yield more accurate first moments of the charge distribution than do the charges provided by other charge models, and they provide a new tool to understand the charge flow in complex systems. The CM5 charge model is extended to solid-state systems, where it is used to describe the charge flow in the delithiation process of lithium-ion batteries.

■ ASSOCIATED CONTENT

Supporting Information

Table for the partial atomic charges on Li atoms with different Li−O−Li angles in singlet Li_2O molecules using various charge models. This material is available free of charge via the Internet at http://pubs.acs.org.

■ AUTHOR INFORMATION

Corresponding Author

*E-mail: truhlar@umn.edu.

Notes

The authors declare no competing financial interest.

■ ACKNOWLEDGMENTS

The authors thank Kaining Duanmu, Laura Fernandez, Sijie Luo, and Pragya Verma for helpful discussions. This work was supported in part by the U.S. Department of Energy, Office of Basic Energy Sciences, under grant no. DE-SC0008662 (charge models in solid-state systems, charge flow during delithiation, and comparison of other approaches to determine charge flow, Sections 4.2 and 4.3) and by the Inorganometallic Catalyst Design Center (comparison of charge models in small molecules, Section 4.1).

■ REFERENCES

(1) Weiner, S. J.; Kollman, P. A.; Case, D. A.; Singh, U. C.; Ghio, C.; Alagona, G.; Profeta, S.; Weiner, P. A new force field for molecular mechanical simulation of nucleic acids and proteins. *J. Am. Chem. Soc.* **1984**, *106*, 765−784.

(2) Wang, J. M.; Wolf, R. M.; Caldwell, J. W.; Kollman, P. A.; Case, D. A. Development and testing of a general amber force field. *J. Comput. Chem.* **2004**, *25*, 1157−1174.

(3) Jorgensen, W. L.; Ulmschneider, J. P.; Tirado-Rives, J. Free energies of hydration from a generalized Born model and an all-atom force field. *J. Phys. Chem. B* **2004**, *108*, 16264−16270.

(4) Fan, Y.; Shi, L. M.; Kohn, K. W.; Pommier, Y.; Weinstein, J. N. Quantitative structure-antitumor activity relationships of camptothecin analogues: Cluster analysis and genetic algorithm-based studies. *J. Med. Chem.* **2001**, *44*, 3254−3263.

(5) Ribeiro, F. A. D.; Ferreira, M. M. C. QSPR models of boiling point, octanol-water partition coefficient and retention time index of polycyclic aromatic hydrocarbons. *J. Mol. Struct.: THEOCHEM* **2003**, *663*, 109−126.

(6) Tishchenko, O.; Li, R.; Truhlar, D. G. Metal-organic charge transfer can produce biradical states and is mediated by conical intersections. *Proc. Nat. Acad. Sci.* **2010**, *107*, 19139−19145.

(7) Lechtken, A.; Neiss, C.; Stairs, J.; Schooss, D. Comparative study of the structures of copper, silver, and gold icosamers: Influence of metal type and charge state. *J. Chem. Phys.* **2008**, *129*, 154304.

(8) Verma, P.; Xu, X. F.; Truhlar, D. G. Adsorption on Fe-MOF-74 for C1-C3 Hydrocarbon Separation. *J. Phys. Chem. C* **2013**, *117*, 12648−12660.

(9) Williams, K. S.; Lenhart, J. L.; Andzelm, J. W.; Bandara, S. V.; Baril, N. F.; Henry, N. C.; Tidrow, M. Z. First principles investigation of water adsorption and charge transfer on III-V(110) semiconductor surfaces. *Surf. Sci.* **2014**, *622*, 71−82.

(10) Wakihara, M.; Yamamoto, O. *Lithium Ion Batteries: Fundamentals and Performance*; Kodansha Wiley: Tokyo, 1998.

(11) Huggins, R. A. *Advanced Batteries: Materials Science Aspects*; Springer: New York, 2009.

(12) Goodenough, J. B.; Kim, Y. Challenges for rechargeable Li batteries. *Chem. Mater.* **2010**, *22*, 587−603.

(13) Etacheri, V.; Marom, R.; Elazari, R.; Salitra, G.; Aurbach, D. Challenges in the development of advanced Li-ion batteries: a review. *Energy Environ. Sci.* **2011**, *4*, 3243−3262.

(14) *Lithium-Ion Batteries: Advanced Materials and Technologies*; CRC Press: Boca Raton, FL, 2011.

(15) Cisneros, G. A.; Karttunen, M.; Ren, P. Y.; Sagui, C. Classical electrostatics for biomolecular simulations. *Chem. Rev. (Washington, DC, U. S.)* **2014**, *114*, 779−814.

(16) Mulliken, R. Electronic population analysis on LCAO-MO molecular wave functions. I. *J. Chem. Phys.* **1955**, *23*, 1833−1840.

(17) Hirshfeld, F. L. Bonded-atom fragments for describing molecular charge-densities. *Theor. Chim. Acta* **1977**, *44*, 129−138.

(18) Momany, F. A. Determination of partial atomic charges from ab initio molecular electrostatic potentials. Application to formamide, methanol, and formic acid. *J. Phys. Chem.* **1978**, *82*, 592−601.

(19) Foster, J. P.; Weinhold, F. Natural hybrid orbitals. *J. Am. Chem. Soc.* **1980**, *102*, 7211−7218.

(20) Storer, J. W.; Giesen, D. J.; Cramer, C. J.; Truhlar, D. G. Class IV charge models: A new semiempirical approach in quantum chemistry. *J. Comput.-Aided Mol. Des.* **1995**, *9*, 87−110.

(21) Li, J. B.; Zhu, T. H.; Cramer, C. J.; Truhlar, D. G. New class IV charge model for extracting accurate partial charges from wave functions. *J. Phys. Chem. A* **1998**, *102*, 1820−1831.

(22) Montgomery, J. A.; Frisch, M. J.; Ochterski, J. W.; Petersson, G. A. A complete basis set model chemistry. VII. Use of the minimum population localization method. *J. Chem. Phys.* **2000**, *112*, 6532−6542.

(23) Gagliardi, L.; Lindh, R.; Karlström, G. Local properties of quantum chemical systems: The LoProp approach. *J. Chem. Phys.* **2004**, *121*, 4494−4500.

(24) Campana, C.; Mussard, B.; Woo, T. K. Electrostatic potential derived atomic charges for periodic systems using a modified error functional. *J. Chem. Theory Comput.* **2009**, *5*, 2866−2878.

(25) Manz, T. A.; Sholl, D. S. Chemically meaningful atomic charges that reproduce the electrostatic potential in periodic and nonperiodic Materials. *J. Chem. Theory Comput.* **2010**, *6*, 2455−2468.

(26) Manz, T. A.; Sholl, D. S. Improved Atoms-in-Molecule Charge Partitioning Functional for Simultaneously Reproducing the Electrostatic Potential and Chemical States in Periodic and Nonperiodic Materials. *J. Chem. Theory Comput.* **2012**, *8*, 2844−2867.

(27) Chen, D. L.; Stern, A. C.; Space, B.; Johnson, J. K. Atomic charges derived from electrostatic potentials for molecular and periodic systems. *J. Phys. Chem. A* **2010**, *114*, 10225−10233.

(28) Marenich, A. V.; Jerome, S. V.; Cramer, C. J.; Truhlar, D. G. Charge Model 5: an extension of Hirshfeld population analysis for the accurate description of molecular interactions in gaseous and condensed phases. *J. Chem. Theory Comput.* **2012**, *8*, 527−541.

(29) Francl, M. M.; Carey, C.; Chirlian, L. E.; Gange, D. M. Charges fit to electrostatic potentials. 2. Can atomic charges be unambiguously fit to electrostatic potentials? *J. Comput. Chem.* **1996**, *17*, 367−383.

(30) Singh, U. C.; Kollman, P. A. An approach to computing electrostatic charges for molecules. *J. Comput. Chem.* **1984**, *5*, 129−145.

(31) Breneman, C. M.; Wiberg, K. B. Determining atom-centered monopoles from molecular electrostatic potentials. The need for high sampling density in formamide conformational analysis. *J. Comput. Chem.* **1990**, *11*, 361−373.

(32) Bader, R. F. W. *Atoms in Molecules: A Quantum Theory*; Oxford University Press: New York, 1990.

(33) Davidson, E. R.; Chakravorty, S. A test of the Hirshfeld definition of atomic charges and moments. *Theor. Chim. Acta* **1992**, *83*, 319−330.

(34) Bultinck, P.; Van Alsenoy, C.; Ayers, P. W.; Carbo-Dorca, R. Critical analysis and extension of the Hirshfeld atoms in molecules. *J. Chem. Phys.* **2007**, *126*, 144111.
(35) Bayly, C. I.; Cieplak, P.; Cornell, W. D.; Kollman, P. A. A well-behaved electrostatic potential based method using charge restraints for deriving atomic charges: the RESP model. *J. Phys. Chem.* **1993**, *97*, 10269−10280.
(36) Laio, A.; VandeVondele, J.; Rothlisberger, U. D-RESP: Dynamically generated electrostatic potential derived charges from quantum mechanics/molecular mechanics simulations. *J. Phys. Chem. B* **2002**, *106*, 7300−7307.
(37) Wang, B.; Truhlar, D. G. Partial Atomic Charges and Screened Charge Models of the Electrostatic Potential. *J. Chem. Theory Comput.* **2012**, *8*, 1989−1998.
(38) Löwdin, P.-O. On the non-orthogonality problem connected with the use of atomic wave functions in the theory of molecules and crystals. *J. Chem. Phys.* **1950**, *18*, 365−375.
(39) Li, J.; Zhu, T.; Cramer, C. J.; Truhlar, D. G. New Class IV Charge Model for Extracting Accurate Partial Charges from Wave Functions. *J. Phys. Chem. A* **1998**, *102*, 1820−1831.
(40) Marenich, A. V.; Cramer, C. J.; Truhlar, D. G. Reduced and quenched polarizabilities of interior atoms in molecules. *Chem. Sci.* **2013**, *4*, 2349−2356.
(41) Kresse, G.; Furthmuller, J. Efficiency of ab-initio total energy calculations for metals and semiconductors using a plane-wave basis set. *Comput. Mater. Sci.* **1996**, *6*, 15−50.
(42) Kresse, G.; Furthmuller, J. Efficient iterative schemes for ab initio total-energy calculations using a plane-wave basis set. *Phys. Rev. B* **1996**, *54*, 11169.
(43) Frisch, M. J.; Trucks, G. W.; Schlegel, H. B.; Scuseria, G. E.; Robb, M. A.; Cheeseman, J. R.; Montgomery, J. A., Jr.; Vreven, T.; Kudin, K. N.; Burant, J. C.; Millam, J. M.; Iyengar, S. S.; Tomasi, J.; Barone, V.; Mennucci, B.; Cossi, M.; Scalmani, G.; Rega, N.; Petersson, G. A.; Nakatsuji, H.; Hada, M.; Ehara, M.; Toyota, K.; Fukuda, R.; Hasegawa, J.; Ishida, M.; Nakajima, T.; Honda, Y.; Kitao, O.; Nakai, H.; Klene, M.; Li, X.; Knox, J. E.; Hratchian, H. P.; Cross, J. B.; Bakken, V.; Adamo, C.; Jaramillo, J.; Gomperts, R.; Stratmann, R. E.; Yazyev, O.; Austin, A. J.; Cammi, R.; Pomelli, C.; Ochterski, J. W.; Ayala, P. Y.; Morokuma, K.; Voth, G. A.; Salvador, P.; Dannenberg, J. J.; Zakrzewski, V. G.; Dapprich, S.; Daniels, A. D.; Strain, M. C.; Farkas, O.; Malick, D. K.; Rabuck, A. D.; Raghavachari, K.; Foresman, J. B.; Ortiz, J. V.; Cui, Q.; Baboul, A. G.; Clifford, S.; Cioslowski, J.; Stefanov, B. B.; Liu, G.; Liashenko, A.; Piskorz, P.; Komaromi, I.; Martin, R. L.; Fox, D. J.; Keith, T.; Al-Laham, M. A.; Peng, C. Y.; Nanayakkara, A.; Challacombe, M.; Gill, P. M. W.; Johnson, B.; Chen, W.; Wong, M. W.; Gonzalez, C.; Pople, J. A. *Gaussian 09*, D.01; Gaussian, Inc.: Wallingford, CT, 2009.
(44) Marenich, A. V.; Cramer, C. J.; Truhlar, D. G. *CM5PAC*; University of Minnesota: Minneapolis, MN, 2013.
(45) Manz, T. A. Chargemol program for performing DDEC analysis, version 2.2 beta, May 25, 2013. ddec.sourceforge.net.
(46) Philipsen, P. H. T.; Velde, G. t.; Baerends, E. J.; Berger, J. A.; Boeij, P. L. d.; Groeneveld, J. A.; Kadantsev, E. S.; Klooster, R.; Kootstra, F.; Romaniello, P.; Skachkov, D. G.; Snijders, J. G.; Wiesenekker, G.; Ziegler, T. *BAND2013*; SCM, Theoretical Chemistry, Vrije Universiteit: Amsterdam, The Netherlands, 2013.
(47) Velde, G. t.; Baerends, E. J. Precise density-functional method for periodic structures. *Phys. Rev. B* **1991**, *44*, 7888−7903.
(48) Wiesenekker, G.; Baerends, E. J. Quadratic integration over the three-dimensional Brillouin zone. *J. Phys.: Condens. Matter* **1991**, *3*, 6721−6742.
(49) Veryazov, V.; Widmark, P. O.; Serrano-Andres, L.; Lindh, R.; Roos, B. O. MOLCAS as a development platform for quantum chemistry software. *Int. J. Quantum Chem.* **2004**, *100*, 626−635.
(50) Aquilante, F.; De Vico, L.; Ferre, N.; Ghigo, G.; Malmqvist, P. A.; Neogrady, P.; Pedersen, T. B.; Pitonak, M.; Reiher, M.; Roos, B. O.; Serrano-Andres, L.; Urban, M.; Veryazov, V.; Lindh, R. Software News and Update MOLCAS 7: The Next Generation. *J. Comput. Chem.* **2010**, *31*, 224−247.
(51) Tang, W.; Sanville, E.; Henkelman, G. A grid-based Bader analysis algorithm without lattice bias. *J. Phys.: Condens. Matter* **2009**, *21*, 084204.
(52) Zhao, Y.; Truhlar, D. G. A new local density functional for main-group thermochemistry, transition metal bonding, thermochemical kinetics, and noncovalent interactions. *J. Chem. Phys.* **2006**, *125*, 194101.
(53) Weigend, F.; Ahlrichs, R. Balanced basis sets of split valence, triple zeta valence and quadruple zeta valence quality for H to Rn: Design and assessment of accuracy. *Phys. Chem. Chem. Phys.* **2005**, *7*, 3297−3305.
(54) Widmark, P. O.; Malmqvist, P. A.; Roos, B. O. Density-matrix Averaged Atomic Natural Orbital (ANO) Basis-sets for Correlated Molecular Wave-functions. 1. 1st Row Atoms. *Theor. Chim. Acta* **1990**, *77*, 291−306.
(55) Roos, B. O.; Lindh, R.; Malmqvist, P. A.; Veryazov, V.; Widmark, P. O. Main group atoms and dimers studied with a new relativistic ANO basis set. *J. Phys. Chem. A* **2004**, *108*, 2851−2858.
(56) Roos, B. O.; Veryazov, V.; Widmark, P. O. Relativistic atomic natural orbital type basis sets for the alkaline and alkaline-earth atoms applied to the ground-state potentials for the corresponding dimers. *Theor. Chem. Acc.* **2004**, *111*, 345−351.
(57) Roos, B. O.; Lindh, R.; Malmqvist, P. A.; Veryazov, V.; Widmark, P. O. New relativistic ANO basis sets for transition metal atoms. *J. Phys. Chem. A* **2005**, *109*, 6575−6579.
(58) Perdew, J. P.; Burke, K.; Ernzerhof, M. Generalized Gradient Approximation Made Simple. *Phys. Rev. Lett.* **1996**, *77*, 3865.
(59) Blochl, P. E. Projector augmented-wave method. *Phys. Rev. B* **1994**, *50*, 17953−17978.
(60) Kresse, G.; Joubert, D. From ultrasoft pseudopotentials to the projector augmented-wave method. *Phys. Rev. B* **1999**, *59*, 1758−1775.
(61) Kresse, G.; Furthmuller, J. Efficient iterative schemes for ab initio total-energy calculations using a plane-wave basis set. *Phys. Rev. B* **1996**, *54*, 11169−11186.
(62) Heyd, J.; Scuseria, G. E.; Ernzerhof, M. Hybrid functionals based on a screened Coulomb potential. *J. Chem. Phys.* **2003**, *118*, 8207−8215.
(63) Chevrier, V. L.; Ong, S. P.; Armiento, R.; Chan, M. K. Y.; Ceder, G. Hybrid density functional calculations of redox potentials and formation energies of transition metal compounds. *Phys. Rev. B* **2010**, *82*, 075122.
(64) Shao-Horn, Y.; Levasseur, S.; Weill, F.; Delmas, C. Probing lithium and vacancy ordering in O3 layered Li_xCoO_2 (x approximate to 0.5) - An electron diffraction study. *J. Electrochem. Soc.* **2003**, *150*, A366−A373.
(65) Ensling, D.; Cherkashinin, G.; Schmid, S.; Bhuvaneswari, S.; Thissen, A.; Jaegermann, W. Nonrigid Band Behavior of the Electronic Structure of $LiCoO_2$ Thin Film during Electrochemical Li Deintercalation. *Chem. Mater.* **2014**, *26*, 3948−3956.
(66) Reed, J.; Ceder, G. Charge, potential, and phase stability of layered $Li(Ni_{0.5}Mn_{0.5})O_2$. *Electrochem. Solid State Lett.* **2002**, *5*, A145−A148.
(67) Miao, S.; Kocher, M.; Rez, P.; Fultz, B.; Ozawa, Y.; Yazami, R.; Ahn, C. C. Local Electronic Structure of Layered $Li_xNi_{0.5}Mn_{0.5}O_2$ and $Li_xNi_{1/3}Mn_{1/3}Co_{1/3}O2$. *J. Phys. Chem. B* **2005**, *109*, 23473−23479.
(68) Geldof, D.; Krishtal, A.; Blockhuys, F.; Van Alsenoy, C. An Extension of the Hirshfeld Method to Open Shell Systems Using Fractional Occupations. *J. Chem. Theory Comput.* **2011**, *7*, 1328−1335.
(69) Zuo, J. M. Measurements of Electron Densities in Solids: a Real-space View of Electronic Structure and Bonding in Inorganic Crystal. *Rep. Prog. Phys.* **2004**, *67*, 2053−2103.